Journal of Medicinal Chemistry

Article

pubs.acs.org/jmc

Structure-Based Selectivity Optimization of Piperidine−Pteridine Derivatives as Potent *Leishmania* Pteridine Reductase Inhibitors

Paola Corona,[‡] Federica Gibellini,[†] Andrea Cavalli,[§,∥] Puneet Saxena,[†] Antonio Carta,[‡] Mario Loriga,[‡] Rosaria Luciani,[†] Giuseppe Paglietti,[‡] Davide Guerrieri,[†] Erika Nerini,[†] Shreedhara Gupta,[⊥] Véronique Hannaert,[⊥] Paul A. M. Michels,[⊥] Stefania Ferrari,*[,†] and Paola M. Costi*[,†]

[†]Dipartimento di Scienze Farmaceutiche, Università degli Studi di Modena e Reggio Emilia, Via Campi 183, 41100 Modena, Italy

[‡]Dipartimento di Chimica e Farmacia, Università degli Studi di Sassari, via Muroni 23/a, 07100 Sassari, Italy

[§]Dipartimento di Scienze Farmaceutiche, Università degli Studi di Bologna, Via Belmeloro, 40126 Bologna, Italy

[∥]Drug Discovery and Development, Istituto Italiano di Tecnologia, via Morego 30, 16163 Genova, Italy

[⊥]Research Unit for Tropical Diseases, de Duve Institute and Laboratory of Biochemistry, Université catholique de Louvain, Avenue Hippocrate 74, Postal Box B1.74.01, B-1200 Brussels, Belgium

Supporting Information

ABSTRACT: The upregulation of pteridine reductase (PTR1) is a major contributor to antifolate drug resistance in *Leishmania* spp., as it provides a salvage pathway that bypasses dihydrofolate reductase (DHFR) inhibition. The structure-based optimization of the PTR1 inhibitor methyl-1-[4-(2,4-diaminopteridin-6-ylmethylamino)benzoyl]-piperidine-4-carboxylate (**1**) led to the synthesis of a focused compound library which showed significantly improved selectivity for the parasite's folate-dependent enzyme. When used in combination with pyrimethamine, a DHFR inhibitor, a synergistic effect was observed for compound **5b**. This work represents a step forward in the identification of effective antileishmania agents.

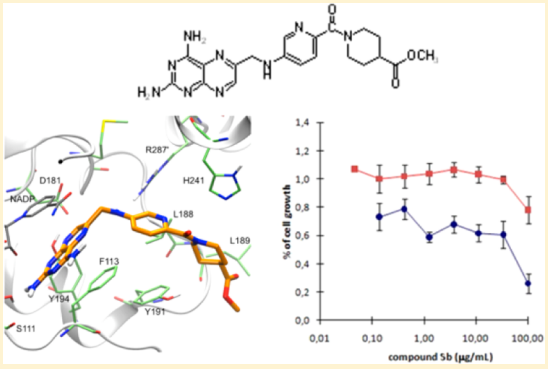

INTRODUCTION

Approximately 350 million people in the tropical and subtropical regions of the world are at risk of contracting forms of the parasitic disease known as leishmaniasis. Its clinical spectrum ranges from the self-healing or scarring cutaneous form to the disfiguring mucocutaneous leishmaniasis and the deadly (if untreated) visceral form. The disease is caused by protists of the genus *Leishmania*; to date, no satisfactory treatment option is available due to high costs, difficulty of administration, and the development of drug resistance.[1,2]

Drugs that target the folate pathway, named antifolates, have been successfully employed against cancer, bacterial infections, certain autoimmune diseases, and malaria, but they have no efficacy against *Leishmania* despite it being a folate auxotroph.[3] The main target of antifolates is the enzyme dihydrofolate reductase (DHFR, E.C. 1.5.1.3), which carries out the progressive reduction of folate to dihydrofolate and then tetrahydrofolate. Reduced folates are employed as cofactors in crucial cellular events such as DNA and protein synthesis and methylation reactions.

Leishmania is able to overcome DHFR inhibition by overexpressing pteridine reductase 1 (PTR1, E.C. 1.5.1.33), an enzyme mainly involved in the reduction of biopterin (first to dihydrobiopterin, then to tetrahydrobiopterin) but that is also able to reduce other pterins and folates. Despite the requirement for reduced biopterin for the growth and survival of *Leishmania major*, PTR1 is not a drug target on its own, likely because of the parasite's ability to scavenge for tetrahydrobiopterin in the phagolysosomes of its host macrophages. For this reason, antifolate therapy could be successfully achieved in *Leishmania* only when both DHFR and PTR1 are simultaneously inhibited by a single drug or by two drugs administered in combination. A successful therapy should not affect the activity of human DHFR (hDHFR). Although the overall protein fold of DHFR is conserved, the primary sequence has diverged considerably among various species through evolution; DHFRs from different organisms show dramatic differences in their inhibition by certain folate analogues.[4] While human DHFR is a monofunctional enzyme, in trypanosomatidic parasites, DHFR and TS activities are expressed as a bifunctional enzyme, dihydrofolate reductase−thymidylate synthase (DHFR-TS), in which the N-terminal DHFR domain is linked to the TS domain. LmDHFR domain share around 25% and 40%, respectively, of identity and similarity with hDHFR; this

Received: April 20, 2012
Published: September 4, 2012

Table 1. Inhibition Constants (K_i) and Selectivity Index (SI) of the Synthesized Compounds; MTX, 1, and 2 Are Reported for Comparison

Code	Structure	$K_{i\ vs\ LmPTR1}$ nM	$K_{i\ vs\ hDHFR}$ nM	$K_{i\ vs\ hTS}$ nM	SI hDHFR/LmPTR1 SI hTS/LmPTR1
MTX	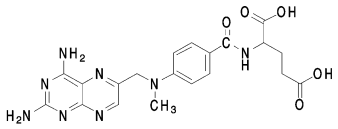	180[a]	3.4 x 10^{-3} [a]	600 ± 33[a]	0 3
1	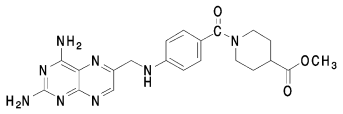	100[a]	10000[a]	NI[a]	100 --
2	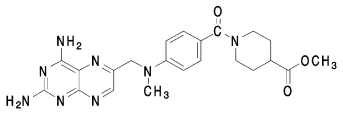	37[a]	800[a]	NI (15 μM)[b]	21 --
5a	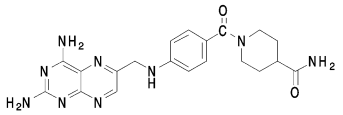	390 ± 24	15430± 2600	NI (15 μM)[b]	39 --
5b	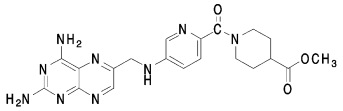	210 ± 15	NI (30 μM)[b]	NI (50 μM)[b]	-- --
5c	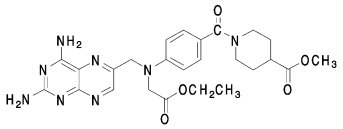	100 ± 4	NI (30 μM)[b]	NI (30 μM)[b]	-- --
5d	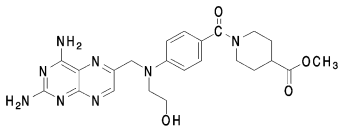	30 ± 2	4330 ± 250	64000± 4300	144 2133
5e	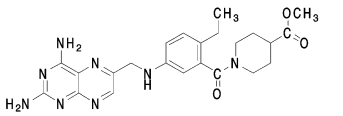	60 ± 4	4680 ± 680	NI (30 μM)[b]	78 --
5f	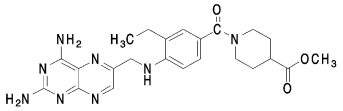	78 ± 4	NI (30 μM)[b]	NI (30 μM)[b]	-- --
6a	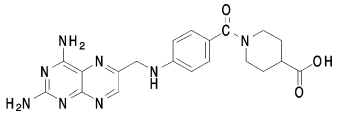	4170 ± 310	590 ± 28	NI (15 μM)[b]	0 --

[a]Already reported in ref 7. [b]NI: no inhibition at the concentration reported in brackets.

suggests that the selective inhibition of LmDHFR with respect to hDHFR could be possible.[5,6]

We previously reported the design, synthesis, and biological evaluation of a novel PTR1 inhibitor (**1**, Table 1) that produced an additive inhibition profile when tested in combination with known DHFR inhibitors such as pyrimethamine (PYR).[7] Compound **1** (Table 1) was shown to be a potent *L. major* PTR1 (LmPTR1) inhibitor with an inhibition constant (K_i) of

dx.doi.org/10.1021/jm300563f | J. Med. Chem. 2012, 55, 8318−8329

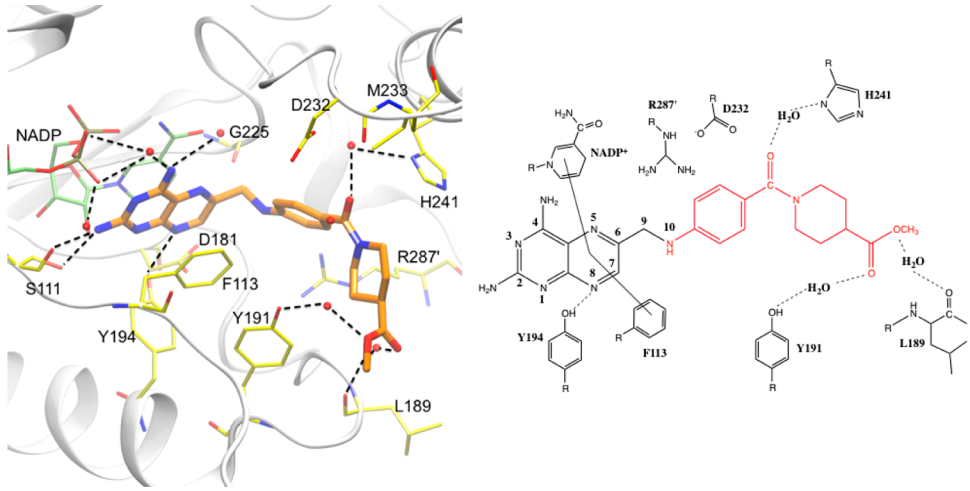

Figure 1. (left) 3D representation of the interactions between compound **1** (orange) and the enzyme's active site residues (in yellow) (PDB ID: 3H4V). Color code: O and N atoms are in red and blue, respectively; C atoms for compound **1** are in orange, whereas of $NADP^+$ and active site residues are in lime and yellow, respectively. The hydrogen bond interactions are shown in broken black lines. Water molecules are shown in red CPK representation. (right) Schematic overview of the interactions are shown where the head region of compound **1** is drawn in black, while the tail region is in red.

100 nM and a selectivity index (Supporting Information, Table 1) over hDHFR of approximately 100. Compound **1** was shown to bind PTR1 (PDB ID 3H4V) in the active site with an orientation that resembled that of the substrate, dihydrobiopterin (PDB IDs 2BF7 and 1E92), rather than that of the archetypal antifolate methotrexate (MTX, PDB ID 1E7W, Figure 1), despite having a similar chemical structure.[7]

Here, seven compounds were designed, synthesized, and tested for their antileishmanial activity both against purified LmPTR1 and on cultured promastigote forms of *Leishmania mexicana* and *L. major*; their synergistic effect in combination with known antifolates was evaluated. Inhibitors of PTR1 are known to make cells more sensitive to oxidative stress by decreasing the intracellular levels of tetrahydrobiopterin, although the mechanistic details are still unclear. Accordingly, the inhibition of PTR1 caused a reduction of the levels of tetrahydrobiopterines, and the parasitic cells became more sensitive to oxidative stress than control cells. This assay represents further confirmation that inhibition of the target enzyme is taking place in the cell.

RESULTS AND DISCUSSION

Design of Compound 1 Analogues. To improve the biological profile of compound **1**, a new structural optimization program was started using the X-ray crystal structure of LmPTR1-**1** (PDB-ID: 3H4V), and visual inspection analysis was performed. In the LmPTR1−**1** complex structure, the inhibitor adopts an orientation similar to that observed for the substrate, with the C7−N8 bond near Asp181 and Tyr194. The headgroup of the inhibitor binds between Phe113 and the nicotinamide ring of the cofactor NADPH and forms hydrogen bonds with Ser111, Tyr194, the phosphate, and ribose components of the cofactor and an ordered water molecule. The tail of compound **1** forms hydrogen bonds through one-water-molecule bridges with Tyr191, His241, and the backbone of Leu189; it also interacts with Asp181, Leu188, Gly225, Asp232, and Met233 (Figure 1).

Numerous hydrogen bonds are formed between the pteridine headgroup of **1**, the cofactor and the surrounding amino acids, as well as ordered water molecules. On the other hand, the analysis of the crystal structure suggests the opportunity to increase and optimize the interactions between PTR1 and the tail region of the inhibitor. By performing a structure-based refinement of lead **1**, we aimed to achieve more productive binding interactions between PTR1 and the inhibitor at the tail region, thereby producing an increase in potency and a decrease in toxicity.

The zone between N10 and Arg287′ is hydrophilic and rich in ordered waters, suggesting that the introduction of short chains carrying hydroxyl groups on N10 should mimic the role of the water interactions. If a 2-hydroxy-ethyl chain is added at N10 (compound **5d**, Table 1), the hydroxyl group could establish interactions with both Arg287′ amino groups (from chain D of the tetramer), Asp181 oxygens, and the Gly225 carbonyl group (Figure 1). With the same aim, compound **5c** (Table 1) was designed.

Exploring the surface clearly revealed the need of an hydrogen bond acceptor on the benzene ring due to its proximity of His241 (Figure 1). A possible solution could be the replacement of the benzenic ring with a pyridine ring (compound **5b**, Table 1) in which the nitrogen atom could accept a hydrogen bond from His241.

The area facing the *p*-amino-benzoic-acid (PABA) group on the opposite site of His241 is particularly wide and lacking in hydrophilic groups. The introduction of an ethyl group on this side of the ring (compounds **5f** and **5e**, Table 1) could establish a hydrophobic interaction with Phe113, Leu229, and Val230 (Figure 1). The space available for ligand binding is quite wide, but this is a particularly flexible zone of the active site (as can be observed by comparing the structures of PTR1 in complex with dihydrobiopterin and MTX); thus, the enzyme should be able to easily optimize the interaction with ligands in this region. The replacement of the terminal ester with a carboxylic group (compound **6a**, Table 1) or an amide (compound **5a**, Table 1) can establish a hydrogen bond with the backbone oxygen of Leu189 (Figure 1).

Synthetic Chemistry. On the basis of the structure-based design, we synthesized compounds **5a−f** and **6a**. The synthesis of the 2,4-diaminopteridine derivatives **5a−f** is shown in Scheme 1, while the preparation of the intermediate amines **4a−f** is

dx.doi.org/10.1021/jm300563f | J. Med. Chem. 2012, 55, 8318−8329

Scheme 1. Scheme of Synthesis of Compounds 5a–f and 6a[a]

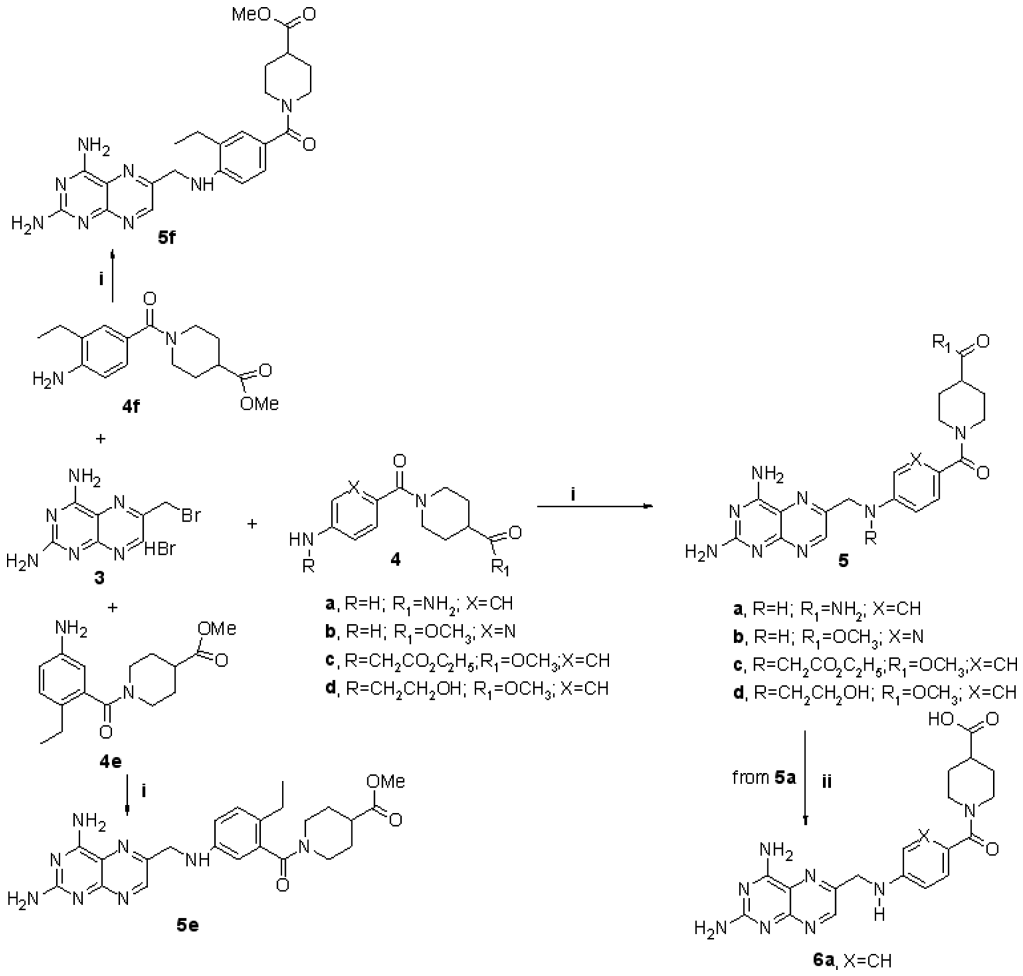

[a]Reagents: (i) DMA, room temperature; (ii) aqueous NaOH.

reported in Schemes 2, 3, 4, and 5 (details are reported in Supporting Information).

Displacement of the bromide of the known 6-(bromomethyl)pteridine-2,4-diamine hydrobromide[8] (**3**) with both the appropriate substituted anilines (**4a,c–f**) and amino picoline derivative (**4b**) was carried out in anhydrous *N,N*-dimethylacetamide (DMA) at room temperature to afford the desired target compounds **5a–f** in yields of 33–65% (Scheme 1).

The acid (**6a**) was obtained by alkaline hydrolysis of the amide (**5a**) with a 92% yield (Scheme 1).

The intermediates **4a**, **4c**, and **4d** were synthesized starting from the 4-nitrobenzoyl chloride (**7**), which was condensed with piperidine-4-carboxamide (**8**) or methyl piperidine-4-carboxylate (**9**) to give the nitro compounds **10** and **11**, respectively (Scheme 2). Reduction of the nitro compounds was accomplished by hydrogen over 10% Pd–C to give the aminoderivatives **4a** and **12**. Alkylation of the latter with ethyl 2-bromoacetate or 2-bromoethanol resulted in the (**4c**) and (**4d**) derivatives, respectively.

Compound **4b** was synthesized by condensation of 5-nitropicolinoyl chloride (**14**) obtained from the parent acid purposely prepared as described,[9] with methyl piperidine-4-carboxylate (**9**) at room temperature in *N,N*-dimethylformamide (DMF) and in the presence of triethylamine (Et_3N) to give the intermediate **15,** which underwent successive hydrogenation (Scheme 3). Compound **4e** was obtained according to the sequence of reactions outlined in Scheme 4, under similar conditions as described above, starting with 2-ethyl-4-nitrobenzoyl chloride (**17**)[10] and the ester (**9**). Finally, the isomer compound (**4f**) was prepared in an identical manner as described above from 3-ethyl-4-nitrobenzoyl chloride (**20**), which was obtained from the known parent acid (**19**)[11] (Scheme 5) and the ester (**9**).

Evaluation of the Inhibition of Enzyme Activity Inhibition and Structure–Activity Relationships. The ability of the designed compounds to inhibit purified LmPTR1 in vitro was compared with their ability to inhibit the purified human folate-dependent enzymes hDHFR and thymidylate synthase (hTS) to estimate their potency and potential toxicity (Table 1).

In vitro evaluation of **5d** validated the design strategy: the addition of the hydroxyethyl chain led to a 3-fold improvement in affinity toward LmPTR1 (K_i from 100 to 30 nM) and a less marked increase in inhibitory activity toward hDHFR (K_i from 10 to 4.33 μM) with respect to compound **1**; overall, the modification caused an increase in both the potency and the selectivity (Table 1). In **5c**, a bulkier ethyl ethanoate substituent was inserted on N10; its affinity toward LmPTR1 with respect to the leading compound **1** did not change, but it completely lost its inhibitory activity toward hDHFR, most likely as a consequence of increased steric clash. Compound **5c** was found

dx.doi.org/10.1021/jm300563f | J. Med. Chem. 2012, 55, 8318–8329

Scheme 2. Scheme of Synthesis of Compounds 4a and 4c−d[a]

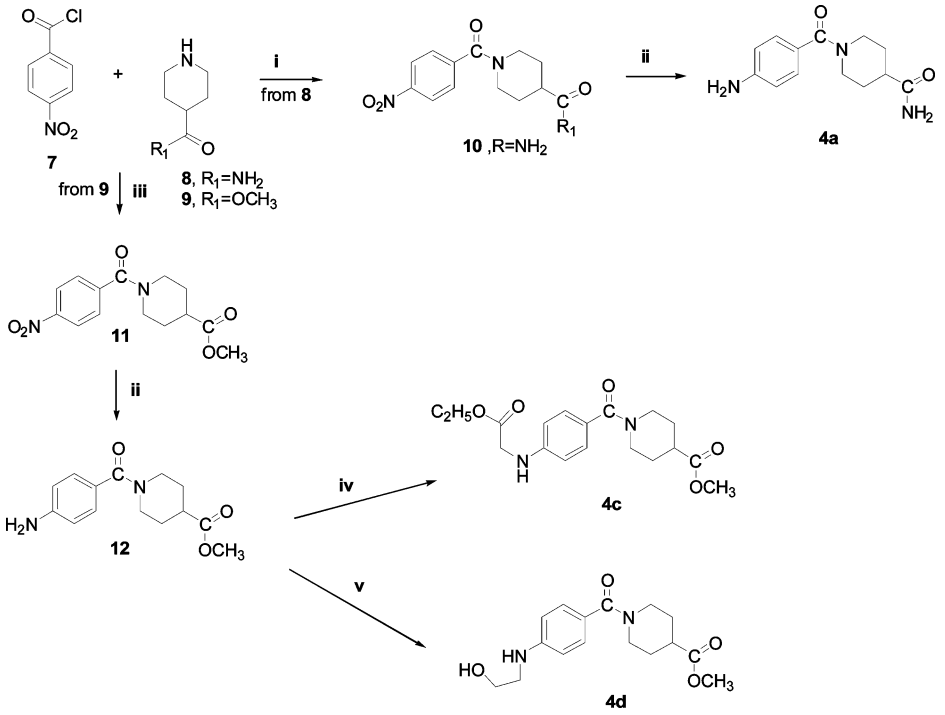

[a]Reagents: (i) $NaHCO_3$ H_2O, 100 °C; (ii) H_2 10% Pd−C, EtOH; (iii) Et_3N, DMF, room temperature; (iv) ethyl 2-bromoacetate, *N*-ethyl-*N*-isopropylpropan-2-amine, anhydrous DMF, under N_2 70 °C; (v) 2-bromoethanol, *N*,*N*-dimethylaniline, under argon, 60 °C.

Scheme 3. Scheme of Synthesis of Compound 4b[a]

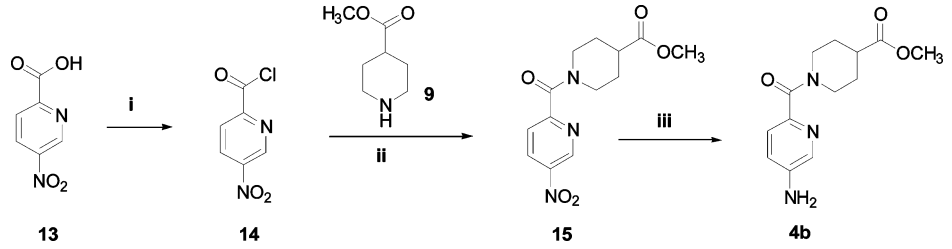

[a]Reagents: (i) $SOCl_2$ 90 °C; (ii) Et_3N, DMF, room temperature; (iii) H_2 10% Pd−C, EtOH.

Scheme 4. Scheme of Synthesis of Compound 4e[a]

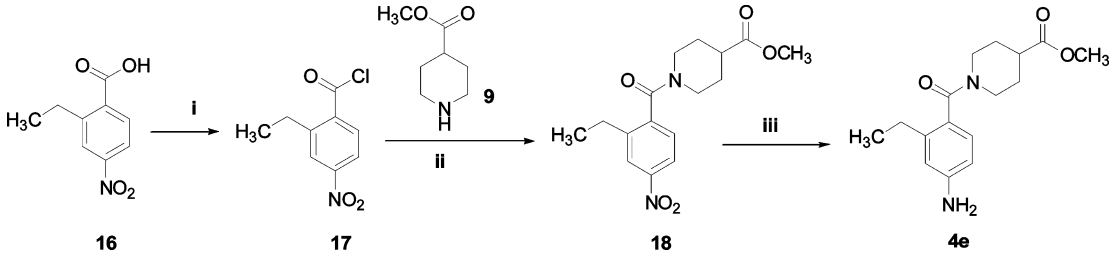

[a]Reagents: (i) $SOCl_2$ 90 °C; (ii) Et_3N, DMF, room temperature; (iii) H_2 10% Pd−C, EtOH.

to be the most selective LmPTR1 inhibitor of the present series and one of the most promising LmPTR1 inhibitors reported by us to date.

Regarding the second set of modifications (**5b**, **5f**, and **5e**), compounds **5f** and **5e** were found to be potent LmPTR1 inhibitors (K_i = 78 and 60 nM, respectively); however, none of them was more potent than **5d** (K_i = 30 nM) and more selective than **5c**, which points to N10 as the most promising position to further explore the present class of compounds. Tail-end modification as in compounds **6a** and **5a** (Table 1) did not lead to an improvement in activity compared to compound **1**.

As a general rule, for a compound to be active on LmPTR1 while possessing a good selectivity over hDHFR, a substitution on N10 with a chain that can interact with hydrophilic residues is required; substitutions of the phenyl ring of PABA that allow hydrophobic interaction with the nonpolar environment of the binding site of hDHFR should be avoided to preserve the selectivity. This is in agreement with our previous analysis of

dx.doi.org/10.1021/jm300563f | J. Med. Chem. 2012, 55, 8318−8329

Scheme 5. Scheme of Synthesis of Compound 4f[a]

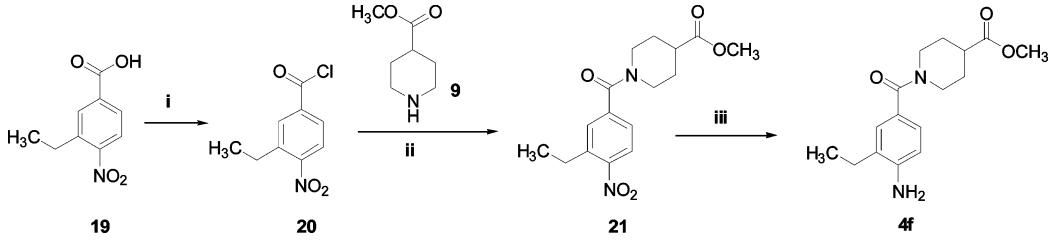

[a]Reagents: (i) $SOCl_2$ 90 °C; (ii) Et_3N, DMF, room temperature; (iii) H_2 10% Pd–C, EtOH.

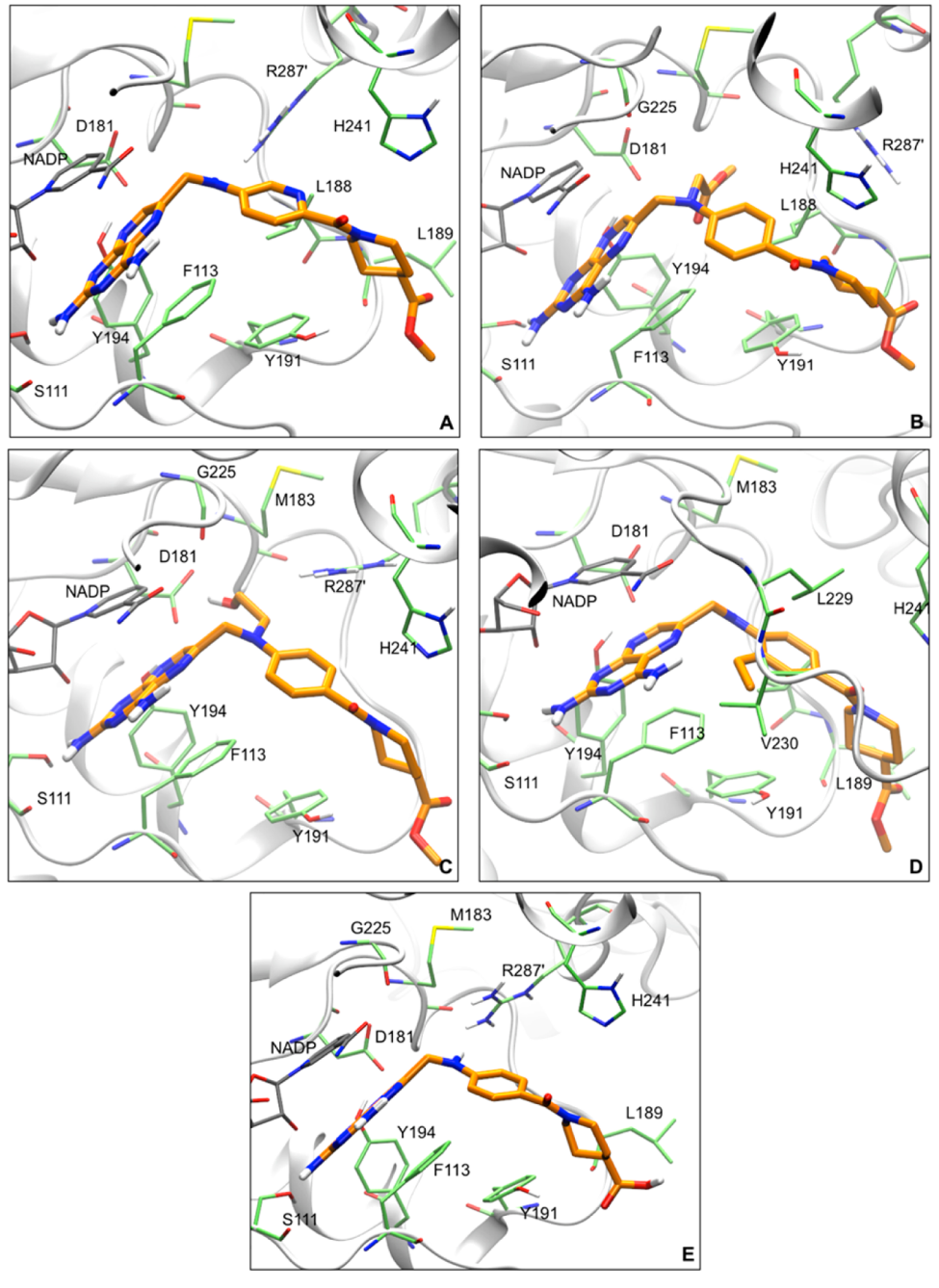

Figure 2. Dockings of the structure-based modifications of lead compound **1** (Figure 1) into the active site of LmPTR1 (PDB ID: 1E92). The ligands (shown in orange) are surrounded by protein's active site residues (shown in licorice, lime color). Color code: O and N atoms are in red and blue, respectively; C atoms for compounds **5b** (A), **5c** (B), **5d** (C), **5f** (D), and **6a** (E) are in orange, whereas for $NADP^+$ and active site residues are in gray and lime, respectively.

dx.doi.org/10.1021/jm300563f | J. Med. Chem. 2012, 55, 8318–8329

compounds **1** and **2**. Whereas compound **1** displayed marked selectivity for LmPTR1, the presence of a methyl group on N10 in compound **2** (instead of a hydrogen atom in **1**) increased the affinity of the molecule for hDHFR (K_i = 800 nM).[7] Like the parent compound, **1**, all compounds, except one, **5d**, do not inhibit hTS. This is in line with MTX profile which is more than 10000-fold less active toward hTS with respect to hDHFR.

Docking Studies. The docking studies were performed to predict the binding modes of the interesting compounds: **5b**, **5c**, **5d**, **5f**, and **6a** versus LmPTR1 with the aim to compare the docking results with the observed inhibition data. To evaluate the correctness of our approach, the docking protocol was first implemented on the available crystallographic structures of compound **1** and MTX and its ability to reproduce the same was tested. The obtained results were found to be in agreement with the experimentally observed binding modes, thereby indicating the validity of the procedure.

The docking result for compound **5b** showed that the nitrogen inserted into the aromatic ring can have a possible interaction with His241 (Figure 2A). Moreover, the rationale behind the synthesis of compound **5c** and **5d** was well corroborated by their docking results. The substitution of acetic acid ethyl ester chain (compound **5c**) made the ligand to interact with Asp181 oxygens. However, the inclusion of the flexibility factor of active residues side chains made Arg187′ (from chain D of the tetramer) move apart due to less availability of space in that region (Figure 2B). Also, the 2-hydroxy-ethyl chain substituted at N10 position of compound **5d** (Figure 2C) was found to orient itself toward the Asp181 oxygens as well as the backbone carbonyl group of Gly225.

The introduction of an ethyl group on the ring helped compound **5f** to establish hydrophobic interaction with Leu229 and Val230. Because of the flexible nature of the side chains, it could be well observed that side chain of Val230 moved in a way (Figure 2D) so as to make enough room for ethyl group substitution. Although the motive behind replacing the terminal ester with carboxylic group (in compound **6a**) was to gain hydrogen bond with the backbone oxygen of Leu189, the expected hydrogen bond could not be observed in the docking result (Figure 2E). Furthermore, from the docking it was also observed that the pteridine ring of the above-mentioned compounds were able to maintain head-to-head stacking interactions between nicotinamide ring of NADP as well as the phenyl ring of Phe113.

A visual inspection of the X-ray structures of the complexes of hDHFR with folic acid or MTX (PDB IDs: 2W3M and 1U72) was helpful in rationalizing the observed SAR. If we reasonably assume that compound **1** can adopt a binding conformation and a binding mode in the active site of hDHFR that is similar to the folate substrate or to the inhibitor MTX (Figure 3), then N10 would sit in a mostly hydrophobic pocket surrounded by Asp21, Leu22, Phe31, Thr56, Ser59, Ile60, and NADPH. It is conceivable that the presence of a methyl group on N10 would dampen its hydrophilic nature and increase the affinity for hDHFR. On the other hand, a bulkier or hydrophilic substituent on N10 could reduce the affinity for hDHFR, thus increasing the selectivity of this compound series toward the parasite's PTR1.

For analyzing the factors contributing to the selectivity of compound **5b** against hDHFR, the docking was used to predict the binding modes of **5b** versus hDHFR. The results were compared with the one obtained vs LmPTR1. The docking results of compound **5b** versus LmPTR1 (PDB ID: 1E92) and hDHFR (PDB ID: 2W3M) showed that the 2,4-diamino-

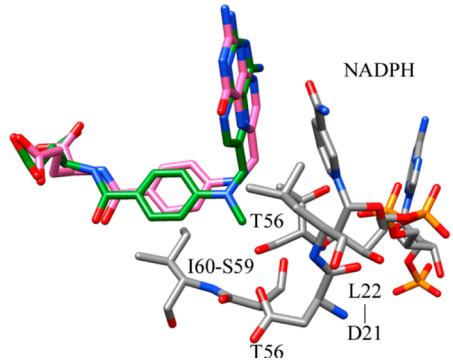

Figure 3. Binding modes of folic acid (C atoms in pink) (PDB ID: 2W3M) and MTX (C atoms in green) (PDB ID: 1U72) with hDHFR (C atoms in gray). All residues and ligands were colored by atom (N in blue, O in red, P in orange); different colors were used for the C atoms to highlight important residues/molecules. Only residues surrounding the N10 position are displayed; most of the residues in the surrounding pocket are hydrophobic: Asp21, Leu22, Thr56, Ser59, Ile60.

pteridine ring of this compound plays an important role in defining its selectivity against hDHFR. On observing the docked pose of **5b** in the active site of LmPTR1 enzyme, the pteridine rings gets firmly sandwiched between the phenyl ring of Phe113 and nicotinamide ring of $NADP^+$ (Figure 4). Such $\pi-\pi$ stacking interaction induces the role of an anchor, giving the compound a firm stability. Apart from this, it also indulges in hydrogen bond formation with Ser111 residue and Tyr194. The 2-amino group makes hydrogen bond with Ser111, whereas the N8 atom of pteridine ring fetches H-bond from hydroxyl group of Tyr194 (Figure 4). All these interactions help the compound gain better activity against LmPTR1.

Although, in the case of hDHFR, the pteridine ring of **5b** is able to occupy region between nicotinamide ring and phenyl ring of Phe34, planarity among them could not be well achieved (Figure 4). Moreover, in the case of hDHFR enzyme, the pteridine rings are able to make only one single hydrogen bond interaction with backbone carbonyl of Ile7 due to relatively poor availability of any hydrogen bond donor atoms in that region. Furthermore, insertion of nitrogen atom in the phenyl ring was well suited for LmPTR1 as it tried to engage interaction with His241, which in the case of hDHFR was not possible due to absence of any such residue.

Antiparasitic Activity. Compounds **5a**–**f** were tested for their antiparasitic activity. As expected (as PTR1 is not a drug target on its own in *Leishmania*[12]), compound **1** and its derivatives were able to inhibit parasite growth only weakly, barely reaching 50% inhibition within the concentration range tested (0.045–100.0 μg/mL). Table 2 and Figure 5 report the growth percentage of both *L. mexicana* and *L. major* exposed to a 50 μg/mL dose of each compound alone or in combination with PYR at 30 μg/mL.

On their own, the compounds induce only limited variations in the *L. mexicana* growth rate, ranging from 111.6% for compound **1** to 88.5% for compound **5a**. Similar results were obtained for *L. major*, where the growth rates ranged from 122.2% for **5d** to 99.6% for **1** (Table 2, Figure 5).

The inhibitors were also tested on *L. mexicana* and *L. major* promastigote lines in combination with the DHFR inhibitor PYR at a fixed concentration. In both cell lines, the compounds were able to considerably enhance PYR activity. Growth rates ranged from 24.4% for the combination **1** + PYR to 12.9% for

dx.doi.org/10.1021/jm300563f | J. Med. Chem. 2012, 55, 8318–8329

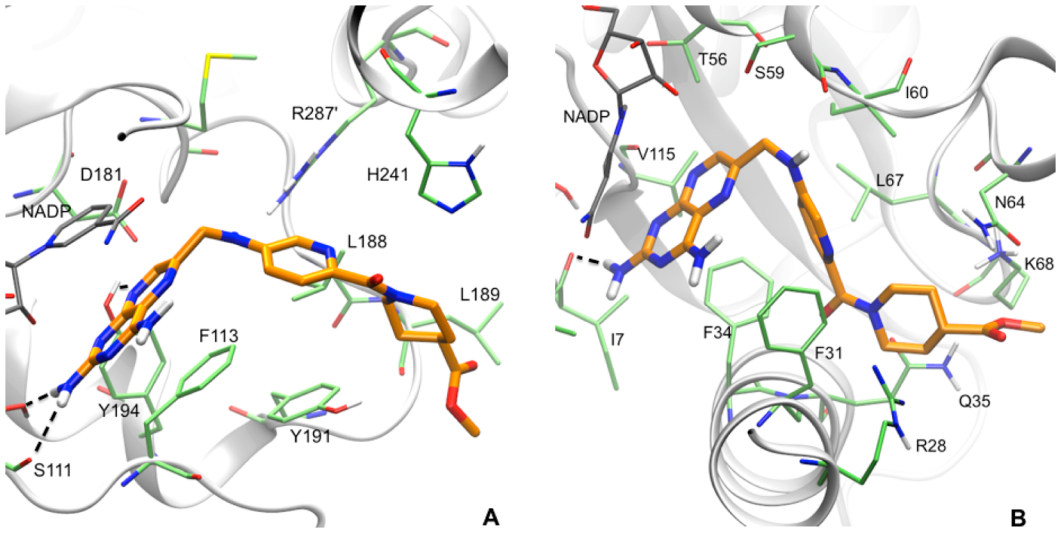

Figure 4. Three-dimensional representation of the interactions made by compound **5b** (licorice, C atoms in orange). The pteridine moiety of **5b** is able to have multiple hydrogen bond interactions (drawn in black dotted lines) with Ser111 and Tyr194 in LmPTR1 (A), whereas in the case of hDHFR (B), the compound is unable to gain any such bindings except Ile7, thereby making it evident that the compound **5b** is well suited for targeting LmPTR1 enzyme with respect to hDHFR. Color code: O and N atoms are in red and blue, respectively; C atoms for compound **5b** are in orange, whereas for $NADP^+$ and active site residues are in gray and lime, respectively, for both the proteins.

Table 2. Effect of Different Compounds, Administered at 50 μg/mL, Alone or Combined with PYR at 30 μg/mL on the Growth of *Leishmania* Promastigotes[a]

compd	growth of *L. mexicana* (%)	growth of *L. major* (%)	ED_{50} of human MRC5 fibroblasts (μg/mL)
PYR	102.5 ± 0.3	68.0 ± 1.2	16.2 ± 2.5
1	111.6 ± 1.4	99.6 ± 1.8	23.4 ± 3.9
1 + PYR	24.4 ± 4.1	30.2 ± 0.53	
5a	88.5 ± 1.4	121.2 ± 1.7	51.0 ± 4.0
5a + PYR	15.7 ± 2.1	47.2 ± 3.7	
5b	95.6 ± 2.1	103.4 ± 1.9	ND[b]
5b + PYR	17.6 ± 0.03	16.1 ± 0.9	
5c	102.3 ± 2.1	100.8 ± 1.8	28% inhibition at 100 μg/mL[c]
5c + PYR	21.9 ± 3.1	37.8 ± 0.3	
5d	100.1 ± 2.1	122.2 ± 2.2	ND[b]
5d + PYR	12.9 ± 2.6	27.4 ± 0.4	
5f	90.6 ± 1.4	104.2 ± 1.8	21.8 ± 0.6
5f + PYR	19.6 ± 1.7	23.1 ± 0.8	

[a]Data are expressed as the percentage of growth compared to control cultures to which no compound had been added. The results obtained for both *Leishmania* and human cells are the mean ± standard deviation obtained in three independent experiments. [b]ND: not determined, i.e., at 50 μg/mL, no inhibition was observed. [c]Little growth inhibition of human MRC5 fibroblasts was obtained at the concentration range tested for **5c**, so no ED_{50} value could be calculated for this compound.

the combination **5d** + PYR for *L. mexicana* and from 47.2% for **5a** + PYR to 16.7% for **5b** + PYR for *L. major* (Table 2, Figure 5). PYR on its own showed a growth rate percentage of 102.3 and 68 at 30 μg/mL, respectively, against *L. mexicana* and *L. major*.

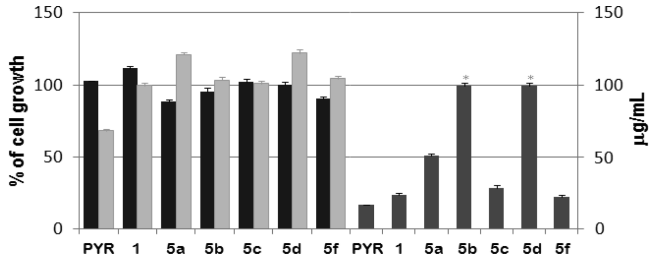

Figure 5. Growth of *L. mexicana* (in black), *L. major* (in light gray) in the presence of 30 μg/mL of PYR or of 50 μg/mL of compounds, left axis; ED_{50} on human fibroblasts (in dark gray), right axis. The growth values are expressed as percentages calculated with respect to the growth of parasites without PYR and pteridine compounds. * not determined, i.e., at 50 μg/mL, no inhibition was observed.

Toxicity of the series has been addressed using cultured MRC-5 human fibroblasts. Most of the compounds appear to be toxic, showing a considerable inhibition of cell growth (ED_{50} values range from 21.8 μg/mL for **5f** to 51.0 μg/mL for **5a**). Notably, no growth inhibition was apparent with **5b** and **5d** in the same concentration range.

Because of the lack of toxicity, **5b** was chosen for a more precise evaluation of its synergistic activity with PYR on *Leishmania* promastigote growth; **1** was also tested as a reference (Figure 6). Parasites were treated with the compounds alone or in combination with PYR (used at its ED_{30} values: 3.5 ± 0.12 μg/mL for *L. major* and 1.78 ± 0.09 μg/mL for *L. mexicana*). The resulting combination indexes, calculated using the Chou−Talalay method[13] were 0.75 for **1** + PYR and 0.80 for **5b** + PYR in *L. major* and 2.05 for **1** + PYR and 1.51 for **5b** + PYR in *L. mexicana*. Values lower than 1 in *L. major* point to a synergistic effect. Data reported in Table 2 were obtained in experiments that had to be performed with parasites grown in culture medium prepared with a new, different batch of serum than the experiments for which data are shown in Figure 6. Although parasite growth and compound effects showed a consistent trend, comparison of absolute numerical values is not

dx.doi.org/10.1021/jm300563f | J. Med. Chem. 2012, 55, 8318−8329

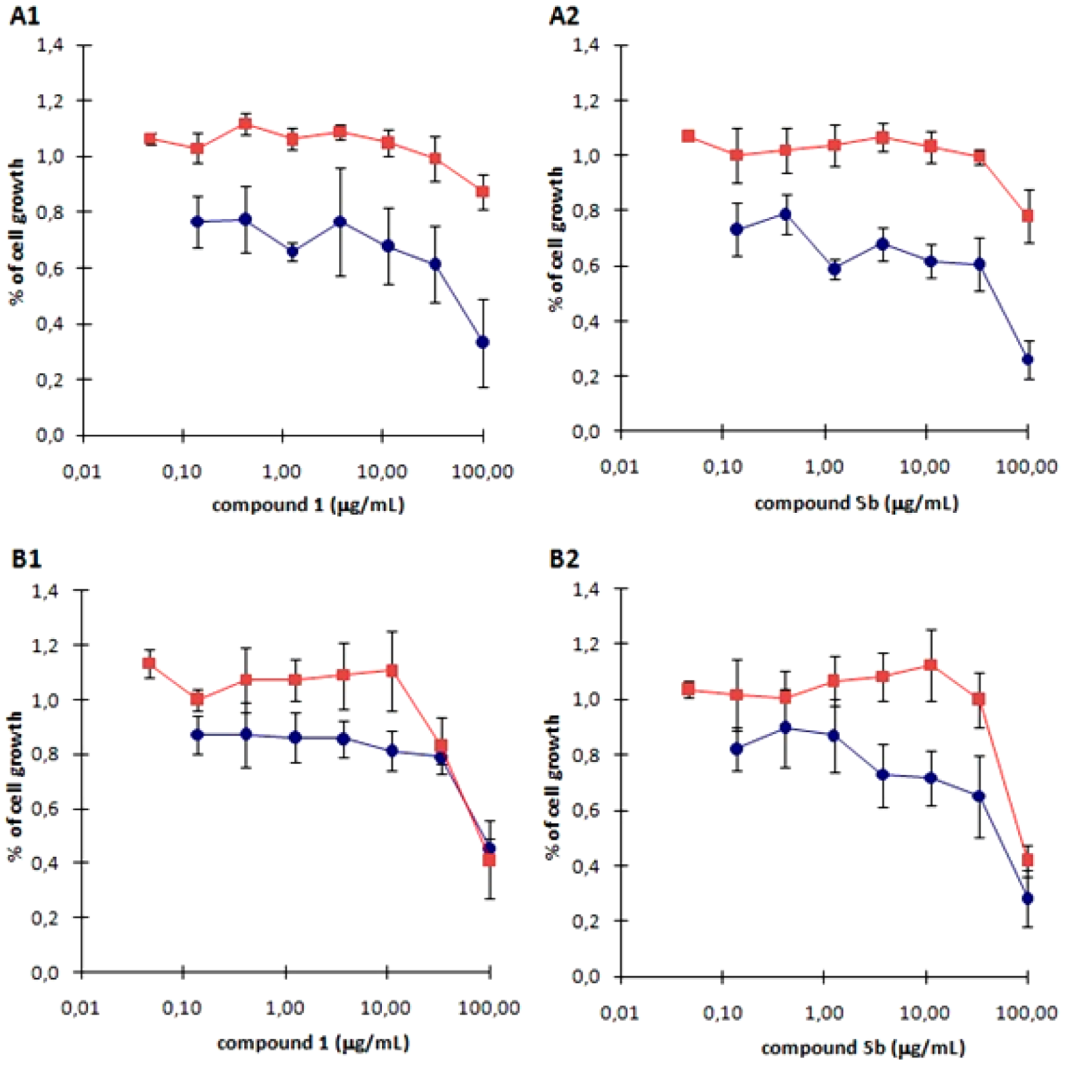

Figure 6. Growth curve of *L. major* (A) and *L. mexicana* (B) promastigotes after exposure to compound **1** (A1 and B1) and compound **5b** (A2 and B2) alone (square dots) or in combination with PYR at its ED_{30} (round dots).

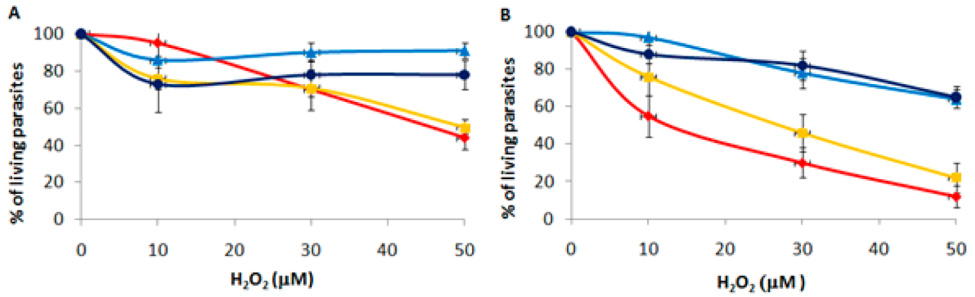

Figure 7. Oxidative stress effect expressed as the percentage of surviving parasites after their exposure to increasing concentrations of H_2O_2 [untreated cells (light blue triangular dots), cells treated with compounds **1** (yellow square dots) and **5b** (red rhomboidal dots), blue round dots represent parasites treated with DMSO alone]. (A) Survival of *L. major* after 45 min of H_2O_2 exposure; (B) survival of *L. mexicana* after 45 min of H_2O_2 exposure.

possible; the results from the different experiments have to be considered independently.

As PTR1 has a well-established role in the resistance of *Leishmania* to oxidative stress,[14] its inhibition could lead to increased sensitivity to oxidant challenges. Promastigotes treated with **1** and **5b** at their ED_{50} in *L. mexicana* and at 100 μg/mL in *L. major* showed a marked reduction in cell survival upon exposure to H_2O_2 compared to untreated parasites exposed to the same concentrations of oxidant (Figure 7). This suggests an impaired ability of the parasites to cope with oxidative stress and is in agreement with the inhibitors being able to target PTR1 in the parasites.[14]

CONCLUSIONS

Our structure-based design and optimization of new inhibitors of LmPTR1 successfully led to the identification of compounds

dx.doi.org/10.1021/jm300563f | J. Med. Chem. 2012, 55, 8318−8329

with an improved binding affinity and selectivity. The compounds were designed to achieve specific interactions with hydrophilic regions of the active site that the precursor, compound **1**, did not exhibit. N10 appeared to be the most promising position for derivatization to enhance the potency of the compounds. Compounds **5c** and **5d** were the best-performing compounds in terms of both potency and selectivity.

The compounds were tested on promastigote-stage cells of the parasite and on MRC-5 human cells to evaluate their antileishmanial activity and toxicity, respectively. The compounds alone did not show appreciable growth inhibition activity, but in combination with the known DHFR inhibitor, PYR, they showed remarkable synergistic activity at the concentration tested. More precisely, **5b** (compared to **1** and to the other derived compounds) showed the best combination of high synergistic inhibitory activity and low toxicity. It showed no toxicity at 50 μg/mL and had parasitic growth inhibition in combination with PYR at 30 μg/mL of 82.4% and 83.9% on *L. mexicana* and on *L. major*, respectively.

The good combination index against *L. major*, the lack of toxicity on human cells, and the ability to impair cell resistance to oxidative stress (which is crucial for these trypanosomatids due to their life-cycle phase occurring in the acidified phagolysosome of macrophages) highlight the potential for these compounds to be developed into more specific clinical agents for counteracting leishmaniasis and other neglected parasitic diseases.

EXPERIMENTAL SECTION

Chemistry. *General Procedures.* All commercially available solvents and reagents were used without further purification. Melting points were measured with a Köfler hot stage or Digital Electrothermal melting point apparatus and are uncorrected. Infrared spectra were recorded as nujol mulls on NaCl plates with a Perkin-Elmer 781 IR spectrophotometer and are expressed in ν (cm^{-1}). UV spectra are qualitative and were recorded in nm for solutions in EtOH with a Perkin-Elmer Lambda 5 spectrophotometer. Nuclear magnetic resonance (^1H, ^{13}C -NMR) spectra were determined in $CDCl_3$, DMSO-d_6, and $CDCl_3$/DMSO-d_6 (1:3 ratio) and were recorded with a Varian XL-200 (200 MHz) spectrometer. Chemical shifts (δ scale) are reported in parts per million (ppm) downfield from tetramethylsilane (TMS) used as an internal standard. Splitting patterns are designated, as follows: s, singlet; a s, apparent singlet; d, doublet; t, triplet; q, quadruplet; m, multiplet; br s, broad singlet; dd, double doublet. The assignment of exchangeable protons (O*H* and N*H*) was confirmed by the addition of D_2O. MS spectra were performed with a combined liquid chromatograph–Agilent 1100 series mass selective detector (MSD). Analytical thin-layer chromatography (TLC) was performed on Merck silica gel F-254 plates. Pure compounds showed a single spot in TLC. For flash chromatography, Merck silica gel 60 was used with a particle size 0.040–0.063 mm (230–400 mesh ASTM). Elemental analyses were performed on a Perkin-Elmer 2400 instrument at the Laboratorio di Microanalisi, Dipartimento di Chimica e Farmacia, Università di Sassari, Italy, and the results were within ±0.4% of theoretical values (Table S1, Table S2 in the Supporting Information). The purity of final products was determined by either elemental analysis or analytical HPLC, and this was more than 95%. The preparation of compounds **4a–f** and **10–12**, **15**, **18**, and **21** are reported in the Supporting Information.

*General Method for the Preparation of 2,4-Diaminopteridine Derivatives **5a–f**.* A mixture of 6-(bromomethyl)pteridine-2,4-diamine hydrobromide (**3**; 0.3 mmol), prepared according to the literature procedure,[8] and an excess of the amines (**4a–f**; 0.6 mmol), synthesized as described in Supporting Information, in DMA (5 mL) was stirred at room temperature until the reaction was complete. The solvent was removed under reduced pressure, and the residue was purified by flash column chromatography using a mixture of chloroform/methanol as the eluent in different ratios. Purification conditions and analytical data are reported below.

*1-(4-((2,4-Diaminopteridin-6-yl)methylamino)benzoyl)-piperidine-4-carboxamide (**5a**).* This compound was prepared in 42% yield by the protocol described in the general procedure starting from **3** and 1-(4-aminobenzoyl)piperidine-4-carboxamide (**4a**) for 7 days; the compound was purified by flash chromatography (chloroform:methanol = 8:2, R_f 0.28) to give a white solid; mp >300 °C. ^1H NMR ($CDCl_3$/DMSO-d_6): δ 8.71 (1H, s, pteridin-H), 7.65 (2H, br s, exc. with D_2O, NH_2), 7.20 (2H, d, J = 8.2 Hz, aryl-H), 6.73 (2H, d, J = 8.8 Hz, aryl-H), 6.64 (1H, br s, exc. with D_2O, NH), 6.34 (2H, s, exc. with D_2O, NH_2), 4.49 (2H, d, J = 4.6 Hz, CH_2), 4.30–4.08 (2H, m, piperidin-H), 3.02–2.90 (2H, m, piperidin-H), 2.60–2.30 (1H, m, piperidin-H), 1.85–1.50 (4H, m, piperidin-H). IR (nujol): ν 3401, 3181, 1645, 1611 cm^{-1}. UV (EtOH): λ_{max} 368, 264, 205 nm. LC/MS: m/z 422 [M + 1].

*Methyl 1-(5-((2,4-Diaminopteridin-6-yl)methylamino)picolinoyl)-piperidine-4-carboxylate (**5b**).* This compound was prepared in 35% yield by the protocol described in the general procedure starting from **3** and methyl 1-(5-aminopicolinoyl)piperidine-4-carboxylate (**4b**) for 7 days; the compound was purified by flash choromatography (chloroform:methanol = 8:2, R_f 0.39) to give a white solid; mp >300 °C. ^1H NMR ($CDCl_3$/DMSO-d_6): δ 8.75 (1H, s, pteridine-H), 8.10 (1H, d, J = 2.4 Hz, picolin-H), 7.73 (2H, br s, exc. with D_2O, NH_2), 7.44 (1H, d, J = 9.0 Hz, picolin-H), 7.11 (1H, dd, J = 8.4 Hz and J = 2.4 Hz, picolin-H), 6.96 (1H, t, exc. with D_2O, NH), 6.40 (2H, s, exc. with D_2O, NH_2), 4.55 (2H, d, J = 4.6 Hz, CH_2), 4.52–4.04 (2H, m, piperidin-H), 3.65 (3H, s, OCH_3), 3.40–2.95 (2H, m, piperidin-H), 2.65–2.50 (1H, m, piperidin-H), 2.04–1.80 (2H, m, piperidin-H), 1.78–1.50 (2H, m, piperidin-H). IR (nujol): ν 3312, 1727, 1590 cm^{-1}. UV (EtOH): λ_{max} 375, 264, 204 nm. LC/MS: m/z 438 [M + 1].

*Methyl 1-(4-(((2,4-Diaminopteridin-6-yl) methyl)(2-ethoxy-2-oxoethyl) amino) benzoyl)piperidine-4-carboxylate (**5c**).* This compound was prepared in 50% yield by the protocol described in the general procedure starting from **3** and methyl 1-(4-(2-ethoxy-2-oxoethylamino) benzoyl) piperidine-4-carboxylate (**4c**) for 7 days; the compound was purified by flash choromatography (chloroform:methanol = 9:1, R_f 0.39) to give a pale yellow solid; mp 143–146 °C.^1H NMR ($CDCl_3$/DMSO-d_6): δ 8.76 (1H, s, pteridin-H), 7.67 (2H, s, exc. with D_2O, NH_2), 7.24 (2H, d, J = 8.0 Hz, aryl-H), 6.69 (2H, d, J = 8.4 Hz, aryl-H), 6.45 (2H, s, exc. with D_2O, NH_2), 4.81 (2H, s, CH_2), 4.38 (2H, s, CH_2), 4.17 (2H, q, J = 6.4, CH_2), 4.22–4.02 (2H, m, piperidin-H), 3.64 (3H, s, CH_3), 3.12–2.92 (2H, m, piperidin-H), 2.65–2.50 (1H, m, piperidin-H), 1.96–1.80 (2H, m, piperidin-H), 1.66–1.46 (2H, m, piperidin-H), 1.25 (3H, t, J = 6.4, CH_3).IR (nujol): ν 3318, 3160, 1731, 1606 cm^{-1}.UV (EtOH): λ_{max} 376, 264, 205 nm.LC/MS: m/z 523 [M + 1].

*Methyl 1-(4-(((2,4-Diaminopteridin-6-yl)methyl)(2-hydroxyethyl)-amino)benzoyl)piperidine-4-carboxylate (**5d**).* This compound was prepared in 57% yield by the protocol described in the general procedure starting from **3** and methyl 1-(4-(2-hydroxyethylamino)-benzoyl)piperidine-4-carboxylate (**4d**) for 7 days; the compound was purified by flash choromatography (chloroform:methanol = 9:1, R_f 0.21) to give a white solid; mp 250–252 °C.^1H NMR ($CDCl_3$/DMSO-d_6): δ 8.59 (1H, s, pteridin-H), 7.52 (2H, s, exc. with D_2O, NH_2), 7.21 (2H, d, J = 8.6 Hz, aryl-H), 6.75 (2H, d, J = 8.6 Hz, aryl-H), 6.44 (2H, br s, exc. with D_2O, NH_2), 4.79 (2H, s, CH_2), 4.15–3.95 (2H, m, piperidin-H), 3.71 (3H, s, CH_3), 3.63 (2H, t partially obscured, CH_2), 3.26 (2H, t partially obscured, CH_2), 3.10–2.90 (2H, m, piperidin-H), 2.70–2.90 (1H, m, piperidin-H), 1.95–1.50 (4H, m, piperidin-H).IR (nujol): ν 3457, 3226, 1732, 1682, 1650, 1604 cm^{-1}.UV (EtOH): λ_{max} 361, 246, 205 nm.LC/MS: m/z 481 [M + 1].

*Methyl1-(5-((2,4-Diaminopteridin-6-yl)methylamino)-2-ethylbenzoyl)piperidine-4-carboxylate (**5e**).* This compound was prepared in 65% yield by the protocol described in the general procedure starting from **3** and methyl 1-(5-amino-2-ethylbenzoyl)-piperidine-4-carboxylate (**4e**) for 7 days; the compound was purified by flash choromatography (chloroform:methanol = :1, R_f 0.30) to give a white solid; mp 197–200 °C.^1H NMR ($CDCl_3$/DMSO-d_6): δ 8.71 (1H, s, pteridin-H), 7.64 (2H, s, exc. with D_2O, NH_2), 7.02 (1H, d, J =

dx.doi.org/10.1021/jm300563f | J. Med. Chem. 2012, 55, 8318–8329

8.2 Hz, aryl-H), 6. 72 (1H, d, J = 8.4 Hz, aryl-H), 6.52 (1H, s, aryl-H), 6.24 (1H, t, exc. with D_2O, NH), 6.17 (2H, br s, exc. with D_2O, NH_2), 4.47 (2H, d, J = 6.4, CH_2), 3.65 (3H, s, CH_3), 3.30−2.80 (4H, m, CH_2 and 2H, piperidin-H), 2.65−2.35 (3H, m, piperidin-H), 2.20−1.40 (4H, m, piperidin-H), 1.13 (3H, t, J = 6.4, CH_3).IR (nujol): ν 3448, 3312, 1732, 1628 cm^{-1}.UV (EtOH): λ_{max} 375, 260, 207 nm.LC/MS: m/z 465 [M + 1].

*Methyl 1-(4-((2,4-Diaminopteridin-6-yl)methylamino)-3-ethylbenzoyl)piperidine-4-carboxylate. (**5f**).* This compound was prepared in 33% yield by the protocol described in the general procedure starting from **3** and methyl 1-(4-amino-3-ethylbenzoyl)-piperidine-4-carboxylate (**4f**) for 7 days; the compound was purified by flash choromatography (chloroform:methanol = 9:1, R_f 0.29) to give a pale-yellow solid; mp 218−220 °C. ^{1}H NMR ($CDCl_3$/DMSO-d_6): δ 8.74 (1H, s, pteridin-H), 7.79 (2H, s, exc. with D_2O, NH_2), 7.38 (2H, s, exc. with D_2O, NH_2), 7.14 (1H, d, J = 2.4 Hz, aryl-H), 7.09 (1H, dd, J = 8.2 Hz and J = 2.4 Hz aryl-H), 6.52 (1H, d, J = 8.2 Hz, aryl-H), 5.83 (1H, br s, exc. with D_2O, NH), 4.60 (2H, s, CH_2), 4.24−4.00 (2H, m, piperidin-H), 3.68 (3H, s, CH_3), 3.10−2.80 (2H, m, piperidin-H), 2.67−2.58 (3H, m, CH_2 and 1H, piperidin-H), 2.10−1.45 (4H, m, piperidin-H), 1.13 (3H, t, J = 7.0, CH_3).IR (nujol): ν 3424, 3315, 1733, 1628 cm^{-1}.UV (EtOH): λ_{max} 375, 260, 207 nm.LC/MS: m/z 465 [M + 1].

*1-(4-((2,4-Diaminopteridin-6-yl)methylamino)benzoyl)-piperidine-4-carboxylic Acid (**6a**).* To a solution of **5a** (0.09 g, 0.21 mmol) in 4 mL of methanol, cooled with an external ice bath, was added an aqueous solution of 1N NaOH (0.67 mL). The mixture was stirred for 20 min. Then stirring was continued at room temperature for an additional 2 h and 45 min. The brown mixture was filtered to remove impurity on suspension. The mother liquors were diluted with 2 mL of water and made acidic with some drops of 6N HCl. After removal of the most methanol under reduced pressure and a few hours standing in the fridge, two portions of 10 mg of acid as a yellow−orange dust were collected. On evaporation in the air of the solvent, a gummy residue was taken up with acetone to give rise to **6a** (80 mg) with an overall yield of 92%; mp >300 °C. ^{1}H NMR (DMSO-d_6): δ 12.15 (1H, br s, COOH), 8.84 (1H, s, pteridin-H), 7.65 (2H, br s, exc. with D_2O, NH_2), 7.21 (2H, d, J = 8.6 Hz, aryl-H), 6.74 (2H, d, J = 8.6 Hz, aryl-H), 6.64 (1H, br s, exc. with D_2O, NH), 6.34 (2H, s, exc. with D_2O, NH_2), 4.52 (2H, a s, CH_2), 4.30−4.08 (2H, m, piperidin-H), 3.02−2.90 (2H, m, piperidin-H), 2.60−2.30 (1H, m, piperidin-H), 1.85−1.50 (4H, m, piperidin-H). IR (nujol): ν 3385 (broad), 3181, 1637 cm^{-1}. UV (EtOH): λ_{max} 388,386, 334, 322, 254 nm. LC/MS: m/z 423 [M + 1].

Enzymology. The proteins were purified as described previously.[7] The folate cofactors and substrates were a gift from Merck Eprova; all other substrates, cofactors, and reagents were purchased from Sigma. LmPTR1, hDHFR, and hTS activities were assessed spectrophotometrically as previously described.[7] Kinetic studies were performed as continuous assays executed in a Beckman DU640 spectrophotometer. K_i values were obtained from IC_{50} (concentration of inhibitor causing 50% enzyme activity inhibition) plots assuming competitive inhibition.[15] The K_i ± standard errors were determined from at least two independent experiments performed in triplicate. Compounds were screened for their activity against LmPTR1, hDHFR, and hTS as previously described.[7] Selectivity indices (SI) were calculated as follow: $SI_{hDHFR/LmPTR1} = K_{i\ hDHFR}/K_{i\ LmPTR1}$; $SI_{hTS/LmPTR1} = K_{i\ hTS}/K_{i\ LmPTR1}$. The DMSO concentration was kept below the concentration affecting enzyme activity (1% for LmPTR1, 5% for hDHFR, 8% for hTS).

Parasitology. *Cell Culture.* Promastigote forms of *L. mexicana* (MHOM/BZ/84/BEL46) and *L. major* (MHOM/SU/73/5-ASKH) were cultured as described earlier.[16] The cultures were initiated at 10^5 parasites/mL, and the cells were harvested in their exponential phase of growth at a density of 2×10^7 parasites/mL.

Parasitic Growth Inhibition. For a first evaluation of the combinatory effect, promastigotes were exposed to high compounds concentrations (50 μg/mL of compound) alone or in combination with PYR at 30 μg/mL; to work with such high concentrations of compounds, parasites were plated at 10^6 cells/mL in a 96-well plate, enabling to perform the experiment on cells that were leaving the exponential growth phase and entering the stationary phase. The percentage growth inhibition that was achieved with a single compound was compared to the one obtained by combining each inhibitor with PYR.

Compounds ED_{50} Evaluation. To estimate the concentrations at which compounds cause 50% inhibition of growth (effective dose, ED_{50}) of cultured *Leishmania* promastigotes, the Alamar Blue micromethod based on monitoring the reducing environment of proliferating cells was employed as previously described.[17] Inhibitor stock solutions were in DMSO. For each compound, dilutions were made in culture medium and added to the parasite cultures, giving a series of concentrations starting from 100 μg/mL downward. The ED_{50} values for compound **5b** were higher than 100 μg/mL; therefore, a specific series of assays was performed, giving a set of concentrations from 500 μg/mL downward. The ED_{50} values were calculated by linear interpolation and were the average of three different experiments each performed in duplicate. The optical density in the absence of compounds was set as the 100% control, whereas the commercial antileishmaniasis drug Amphotericin B was used as a positive control.

Synergistic Activity with PYR. The linear interpolation procedure described above has been used to calculate the ED_{30} values (estimated concentrations at which compounds cause 30% inhibition of growth) of PYR in *L. major* and *L. mexicana*. These values have been used to assess the leishmanicidal effect of our compounds and PYR combined: the Alamar Blue micromethod described above was modified, and each sample was added at a series of concentrations of our compounds (from 100 μg/mL downward) and a fixed EC_{30} concentration of PYR. Samples with only PYR were taken as the 100% control. The synergistic effect of PYR combined with the additional compound on *Leishmania* growth was calculated using the combination index, following the Chou−Talalay method.[13]

Oxidative Stress Evaluation. Parasites were plated at 10^5 cells/mL in a 24-well plate, and the compounds were added at their ED_{50} doses for 48 h at 28 °C in *L. mexicana* experiments. In *L. major* experiments, compounds **1** and **5b** were added at 100 μg/mL due to the very high ED_{50}. Subsequently, cells were diluted to 2×10^4 cells/mL and subjected to H_2O_2 treatment for 45 min. Surviving motile parasites were counted using a Neubauer counting grid on an invertoscope. The results are expressed as a series of percentages, taking the compound-treated, non-H_2O_2 exposed sample as the 100% control for each compound treatment. This series was compared with a series of untreated, H_2O_2-exposed samples.

Toxicity Test. The human fibroblast cell line MRC-5 was used to determine the possible toxicity of the compounds in human cells. The culture and toxicity assays were performed using essentially the same method as described previously.[18] In brief, the fibroblasts were cultivated at 37 °C in DMEM medium (Gibco) in the presence of 10% heat-inactivated FBS and extra glutamine in humidified incubators with an atmosphere of 5% CO_2. Cells were seeded to each well of the microplates at a density such that, after 72 h of incubation, adhesive cells had formed a confluent monocellular film in the control wells. After 72 h, Alamar Blue was added and the optical density was measured.

Docking Studies. The docking simulations were performed using the crystallographic structure of LmPTR1 in complex with the cofactor NADP and the substrate dihydrobiopterin (PDB ID: 1E92). The rationale behind choosing this X-ray structure was that it displayed the highest resolution of 2.20 Å among all the available structures of this protein. However, to continue our study, the dihydrobiopterin molecule was removed from the active site and our target compounds were docked in place of it. The docking was performed using the Lamarckin genetic algorithm, which is a subutility available in Autodock software version 4.0.5.[19] Prior to the starting of docking our target compounds, the accuracy of the algorithm was validated by verifying its ability to reproduce the published crystallographic binding conformations of compound **1** (PDB ID: 3H4V) and MTX (PDB ID: 1E7W). Thereafter, an initial population of random individuals was used with a population size of 150 individuals. A maximum number of energy evaluations count was set to be 2500000, and the value of the highest number of generations was kept as 27000. The number of individuals that automatically survive into the next generation (i.e., the elitism

value) was kept 1; the probability that a gene would mutate was set to 0.02. Moreover, the probability that 2 individuals could get crossover was 0.8. Also, the proportional selection criteria was used, where the average of the worst energy was calculated over a window size of 10 generations. The pseudo Solis and Wets local search method was implemented during the docking and the maximum number of iterations per local search was set to 300; the probability of performing a local search on an individual in the population was used as 0.06. The maximum number of consecutive successes or failures before doubling or halving the local search step size (P, ρ) was 4 in both cases, where the lower bound value on ρ was 0.01.

During the ligand binding procedure, it is very common that the binding might induce some conformational changes in the active site pocket. So, to hold our docking calculations accountable, side chain flexibility criteria was also included, where the side chains of the residues in the vicinity of the active region (Ser111, Phe113, Asp181, Leu189, Tyr191, Tyr194, Asp232, and His241 of chain A and Arg287′ of chain D of tetramer were allowed to move, keeping their backbone fixed.

For analyzing the factors contributing to the selectivity of compound **5b** against hDHFR (PDB ID: 2W3M), all the above parameters were kept the same while performing the docking, except owing to the different active site topology, in this case, side chain flexibility was included for the active site residues: Ile7, Leu22, Arg28. Phe31, Phe34, Gln35, Ile60, Asn64, Leu67, Lys68, and Tyr121 of chain A.

This methodology allowed us to sample their flexible conformations, keeping the ligand binding simultaneously into consideration.

■ ASSOCIATED CONTENT

Supporting Information

Elemental analyses of compounds **5a–f** and **6a**; elemental analyses of intermediates **4a**, **10**, **4b**, **15**, **4c**, **4d**, **12**, **11**, **4e**, **18**, **4f**, and **21**; ^{13}C NMR spectra of compounds **5a–f** and **6a**. This material is available free of charge via the Internet at http://pubs.acs.org.

■ AUTHOR INFORMATION

Corresponding Author

*For M.P.C.: phone, 0039-059-205-5143; fax, 0039-059-205-5131; E-mail, mariapaola.costi@unimore.it. For S.F.: phone, 0039-059-205-5125; fax, 0039-059-205-5131; E-mail, stefania.ferrari@unimore.it.

Author Contributions

The manuscript was written through contributions of all authors. All authors have given approval to the final version of the manuscript.

Notes

The authors declare no competing financial interest.

■ ACKNOWLEDGMENTS

We gratefully acknowledge the support of the Italian Internationalization Programme (2008-2010) and Cassa di Risparmio di Modena Internationalization Programme (Kineto-drugs project, 2008-2010), PRIN2009, and WHO A50599 to M.P.C.

■ ABBREVIATIONS USED

DHFR, dihydrofolate reductase; ED_{30}, effective dose at which compounds cause 30% inhibition of growth; ED_{50}, effective dose at which compounds cause 50% inhibition of growth; hDHFR, human dihydrofolate reductase; hTS, human thymidylate synthase; K_i, inhibition constant; LmPTR1, *Leishmania major* pteridine reductase; MTX, methotrexate; PABA, *p*-aminobenzoic acid; PTR1, pteridine reductase; PYR, pyrimethamine

■ REFERENCES

(1) Ready, P. D. Leishmaniasis emergence in Europe. *Euro Surveill.* **2010**, *15*, 19505–19515. Available online http://www.eurosurveillance.org/ViewArticle.aspx?ArticleId=19505.

(2) Palatnik-de-Sousa, C. B.; Day, M. J. One Health: The global challenge of epidemic and endemic leishmaniasis. *Parasites Vectors* **2011**, *4*, 197–206.

(3) Cunningham, M. L.; Beverley, S. M. Pteridine salvage throughout the *Leishmania* infectious cycle: implication for antifolate chemotherapy. *Mol. Biochem. Parasitol.* **2001**, *113*, 199–213.

(4) Senkovich, O.; Schormann, N.; Chattopadhyay, D. Structures of dihydrofolate reductase–thymidylate synthase of *Trypanosoma cruzi* in the folate-free state and in complex with two antifolate drugs, trimetrexate and methotrexate. *Acta. Crystalogr., Sect. D: Biol. Crystallogr.* **2009**, *65*, 704–716.

(5) Knighton, D. R.; Kan, C.-C.; Howland, E.; Janson, C. A.; Hostomska, Z.; Welsh, K. M.; Matthews., D. A. Structure of and kinetic channelling in bifunctional dihydrofolate reductase–thymidylate synthase. *Nature Struct. Biol.* **1994**, *1*, 186–194.

(6) Zuccotto, F.; Martin, A. C. R.; Laskowski, R. A.; Thornton, J. M.; Gilbert, I. H. Dihydrofolate reductase: a potential drug target in trypanosomes and leishmania. *J. Comput.-Aided Mol. Des.* **1998**, *12*, 241–257.

(7) Cavazzuti, A.; Paglietti, G.; Hunter, W. N.; Gamarro, F.; Piras, S.; Loriga, M.; Allecca, S.; Corona, P.; McLuskey, K.; Tulloch, L.; Gibellini, F.; Ferrari, S.; Costi, M. P. Discovery of potent pteridine reductase inhibitors to guide antiparasite drug development. *Proc. Natl. Acad. Sci. U.S.A.* **2008**, *105*, 1448–1453.

(8) Piper, J. R.; Montgomery, J. A. Preparation of 6-(Bromomethyl)-2,4-pteridinediamine Hydrobromide and Its Use in Improved Syntheses of Methotrexate and Related Compounds. *J. Org. Chem.* **1977**, *42*, 208–211.

(9) Schneider, M.; Harris, T. M. Synthesis of DL-Slaframine. *J. Org. Chem.* **1984**, *49*, 3681–3684.

(10) Reimschneider, R.; Kassahn, H.-G. Acylderivate cyclischer Verbindungen, V. Zur Herstellung von *o*-Diacetyl-benzol und 4-Nitro-1.2-diacetyl-benzol. *Chem. Ber.* **1959**, *92*, 1705–1709.

(11) Bühler, S.; Lagoja, I.; Giergrich, H.; Stengele, K. P.; Pfleiderer, W. New Types of Very Photolabile Protecting Groups Based upon the [2-(2-Nitrophenyl)propoxy]carbonyl (NPPOC) Moiety. *Helv. Chim. Acta* **2004**, *87*, 620–659.

(12) Sienkievikz, N.; Ong, H. B.; Fairlamb, A. H. *Trypanosoma brucei* pteridine reductase 1 is essential for survival in vitro and for virulence in mice. *Mol. Microbiol.* **2010**, *77*, 658–671.

(13) Chou, T. C. Theoretical basis, experimental design, and computerized simulation of synergism and antagonism in drug combination studies. *Pharmacol. Rev.* **2006**, *58*, 621–681.

(14) Papadopoulou, B; Roy, G; Ouellette, M. A novel antifolate resistance gene on the amplified H circle of *Leishmania*. *EMBO J.* **1992**, *11*, 3601–3608.

(15) Segel, I. H. Enzyme Kinetics. *Behaviour and Analysis of Rapid Equilibrium and Steady-State Enzyme Systems*; Wiley Classic Library: New York, 1975.

(16) Brun, R.; Schönenberger, M. Cultivation and in vitro cloning of procyclic forms of *Trypanosoma brucei* in a semi-defined medium. *Acta Trop.* **1979**, *36*, 289–292.

(17) Mikus, J.; Steverding, D. A simple colorimetric method to screen drug toxicity against *Leishmania* using the dye Alamar Blue. *Parasitol. Int.* **2000**, *48*, 265–269.

(18) Ferrari, S.; Morandi, F.; Motiejunas, D.; Nerini, E.; Henrich, S.; Luciani, R.; Venturelli, A.; Lazzari, S.; Calò, S.; Gupta, S.; Hannaert, V.; Michels, P. A.; Wade, R. C.; Costi, M. P. Virtual screening identification of nonfolate compounds, including a CNS drug, as antiparasitic agents inhibiting pteridine reductase. *J. Med. Chem.* **2011**, *54*, 211–221.

(19) Morris, G. M.; Goodsell, D. S.; Halliday, R. S.; Huey, R.; Hart, W. E.; Belew, R. K.; Olson, A. J. Automated Docking Using a Lamarckian Genetic Algorithm and and Empirical Binding Free Energy Function. *J. Comput. Chem.* **1998**, *19*, 1639–1662.